ISSN 1063-7842, Technical Physics, 2007, Vol. 52, No. 7, pp. 911–919. © Pleiades Publishing, Ltd., 2007.
Original Russian Text © N.A. Vinokurov, B.A. Knyazev, G.N. Kulipanov, A.N. Matveenko, V.M. Popik, V.S. Cherkassky, M.A. Shcheglov, 2007, published in Zhurnal Tekhnicheskoĭ Fiziki, 2007, Vol. 77, No. 7, pp. 91–100.

OPTICS, QUANTUM ELECTRONICS

Visualization of Radiation from a High-Power Terahertz Free Electron Laser with a Thermosensitive Interferometer

N. A. Vinokurov, B. A. Knyazev, G. N. Kulipanov, A. N. Matveenko, V. M. Popik, V. S. Cherkassky, and M. A. Shcheglov

Budker Institute of Nuclear Physics, Siberian Division, Russian Academy of Sciences, pr. Akademika Lavrent'eva 11, Novosibirsk, 630090 Russia

Novosibirsk State University, ul. Pirogova 2, Novosibirsk, 630090 Russia

e-mail: knyazev@inp.nsk.su

Received August 23, 2006

Abstract—A thermosensitive interferometer based on a plane-parallel glass plate is used for visualization of a high-power terahertz radiation. The plane wavefront of visible radiation emitted by a semiconductor laser is reflected from the two surfaces of the plate and forms on a screen an interference pattern recorded by a digital video camera. Terahertz radiation being measured is incident on the outer surface of the plate and heats a thin surface layer, which causes a shift of interference fringes. For K8 glass, a shift by one fringe corresponds to an absorbed energy of 5.1 J/cm^2. The problem of determining the sign of the phase shift was solved by comparing the interference patterns with the images obtained with an infrared imager sensitive to near IR radiation. The processing of interference patterns makes it possible to determine the power density distribution over the beam cross section of the Novosibirsk free electron laser. In these measurements, the absolute value of the beam power determined by integrating over the cross section was 65 ± 7 W for a 130-μm wavelength. Visualization of the complex image with a spatial resolution no worse than 1 mm and a frame repetition rate of 25 Hz is demonstrated.

PACS numbers: 07.57.-c, 42.30.Va, 42.25.Hz

DOI: 10.1134/S1063784207070134

INTRODUCTION

The construction of radiation sources in the frequency range 1–10 THz (corresponding to wavelengths from 30 to 300 μm) in recent years has stimulated interest in recording images in this spectral range [1]. The photon energy in this range is 24.0–2.4 meV; i.e., radiation is "not ionizing," which means that "individual" detection of photons requires the application of highly intricate methods (see, for example, [2]), which can hardly become standard. For such a low photon energy, the interaction of radiation with matter in most cases is successfully described by the classical theory of electromagnetic waves. For this reason, radiation in this spectral range is usually detected and visualized using the methods typical of photonics rather than electronics (i.e., with the help of bolometers, photoconducting antennas, and nonlinear optical crystals).

Until recently, all sources of terahertz radiation (both wide-band and monochromatic) had an extremely low average power (although the pulse power could be quite high). For this reason, either sample scanning by a focused terahertz beam or prolonged exposure was required for visualization of images. A detailed description of various available methods for image recording is given in the review [1].

The free electron terahertz laser commissioned in Novosibirsk two years ago [3] generates radiation with an average power of up to 400 W, which exceeds the power of all sources available in this range by 4–5 orders of magnitude. Such a high power makes it possible to use completely new methods for visualization of terahertz radiation.

In this article, we describe a visible-range interferometer based on a plane-parallel glass plate, which makes it possible to visualize radiation fluxes for which the plate is opaque due to the thermooptical effect and to measure the absolute values of the radiation power distribution.

EXPERIMENTAL SETUP

The design of the Novosibirsk free electron laser (FEL) is described in [3]. Laser radiation emerging from an 8-mm aperture in the output mirror of the cavity is transmitted with the help of a system of mirrors via a 13-m optical channel from the radiation danger-

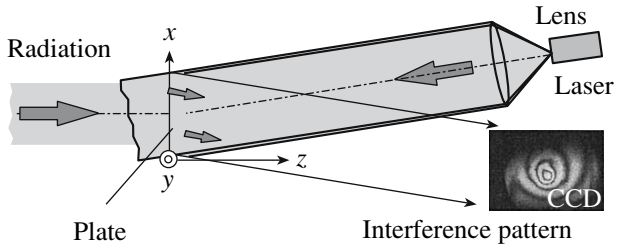

Fig. 1. Schematic diagram of a thermosensitive interferometer.

ous room to the workstation room. To eliminate radiation absorption by water vapor, the optical channel is filled with dry nitrogen and is separated from the atmosphere by a polyethylene or polypropylene film fixed at the outlet. The experiments described below were performed at an average radiation power of up to 100 W. Laser generates a continuous train of 50-ps pulses with a pulse repetition rate of 5.6 MHz. The radiation wavelength can be smoothly tuned from 120 to 235 μm.

The experimental equipment was mounted on an optical bench installed at the optical channel outlet. The characteristic optical path length in air was 50–100 cm in various experiments; for this reason, a part of radiation at certain wavelengths could be absorbed by water vapor whose absorption spectrum in the wavelength under investigation can be found, for example, in [4]. As an aid of visualization of terahertz radiation, we used a SVIT thermograph [5] designed at the Institute of Semiconductor Physics, Siberian Division, Russian Academy of Sciences. It is sensitive to radiation in a range of 2.6–3.0 μm and makes it possible to record a thermal image in the form of a film with a frame repetition rate of 25 Hz. Heating of the plate by terahertz radiation leads to emission from its surface in the near IR range, which is projected to the InAs matrix of the thermograph by a lens cooled to the nitrogen temperature. The surface temperature distribution is recorded in a 128 × 128-pixel file. Knowing the temperature of the surface, it is basically possible to solve the inverse thermal conductivity problem [6, 7] to reconstruct the absolute radiation power distribution; however, this method is insufficiently reliable due to its complexity. In view of the relatively small number of elements in the matrix and a quite high transverse thermal conductivity of the screen, the resolution of the thermograph leaves much to be desired. The time resolution in thermography is determined by the thermal relaxation time and is on the order of 1–2 s. However, the thermograph is very convenient for tracing and monitoring of teraherz radiation and was used in our experiments as an aid for observation and for determining the phase shift sign in the processing of interference patterns (see below).

For recording the absolute distribution of the terahertz radiation power density, a thermosensitive interferometer (TSI) was constructed. Its prototype is the interferometer used for detecting thermal fluxes to the wall in gasdynamic experiments [8]. Figure 1 shoes the schematic diagram of an interferometer analogous to the Fizeau interferometer [9]. Teraherz radiation being studied is absorbed in a plane-parallel K8 glass plate from the 20-mm thick OSK-2TsL optical bench 146 mm in diameter. A plane electromagnetic wave formed by a single-mode semiconductor laser (λ = 665 nm) and 1.5-m lens from the optical bench is incident on the plate at a small angle. After reflection from the front and rear surface of the glass plate, two waves form an interference pattern on the screen.

Interference patterns were recorded by a Sony CDR-TRV230E digital video camera with a frame rate of 25 Hz, which determined the time resolution. Since the glass is opaque in a wavelength range of 2.8–3.0 μm, we simultaneously recorded the image of the "temperature" field of the glass surface with the thermograph.

OPERATION PRINCIPLE OF A THERMOSENSITIVE INTERFEROMETER

If a plane wavefront from a probe laser is incident on a plane-parallel glass plate of thickness L at a certain angle θ, the rays reflected from the front and rear surfaces of the plate are characterized by the optical path difference

$$\varphi_0 = \frac{2\pi nL}{\lambda_0}A + \pi, \tag{1}$$

where n is the refractive index of the plate, λ_0 is the wavelength of the probe laser, and

$$A = \sqrt{1 - \frac{\sin^2\theta}{n^2}}. \tag{2}$$

The rated planeness of the plate used in our experiments is 0.5λ; consequently, in the absence of thermooptical distortions, the "zero field" is not quite uniform.

Let us determine (see [8]) the variation of the optical path difference for the probe laser beam for an arbitrary temperature variation in the plate along the beam. In our calculations, we assume that the angle of incidence of probe radiation is zero (θ = 0). The results of calculations can subsequently be easily corrected by introducing into the corresponding expressions the correction factor

$$\zeta = \frac{n}{n^2 - \sin^2\theta}, \tag{3}$$

which takes into account the increase in the path length in the heated surface layer of the plate. We assume that the time of plate exposure to terahertz radiation is quite short so that only a thin surface layer of the glass plate is heated during the time of measurement. This ensures

a high spatial resolution and makes it possible to disregard transverse heat fluxes.

We denote differentiation with respect to spatial coordinates and time by symbols d and δ, respectively. The optical path difference acquired by test radiation on a segment dl, where the differential is associated with the elementary material layer of the plate, after double passage through the plate is

$$dS(t) = 2n(T(l,t))dl. \quad (4)$$

Its variation over time interval δt is

$$\delta[dS(t)] = \frac{dS(t+\delta t) - dS(t)}{\delta T}\delta T = \frac{\partial dS(t)}{\partial T}\delta T. \quad (5)$$

Substituting relation (4) into this expression and differentiating the result, we obtain the expression

$$\delta[dS(t)] \approx 2(\beta + \alpha n)\delta T(t)dl, \quad (6)$$

correct to second-order terms, where α is the linear expansion coefficient for glass and $\beta = \partial n/\partial T$. Integrating Eq. (6) over the entire path length and multiplying the numerator and denominator by $\rho c_p \lambda_0 \delta t$, we obtain

$$\frac{\delta S}{\lambda_0 \delta t} = \frac{\delta N}{\delta t} = \frac{2(\beta + \alpha n)}{\lambda_0 c_p \rho}\int_L \frac{\delta q(l)dl}{\delta t}. \quad (7)$$

Here, δN is the shift of interference fringes (a certain rational number) at a given point on the plate surface over time interval δt, ρ and c_p are the density and specific heat of glass, δq is the local increment of the thermal energy per unit volume, and the integral is the energy flux $Q(x, y)$ of radiation being measured, which is absorbed by the plate. It can be seen that

$$Q(x, y) = \frac{\delta N}{\delta t}K, \quad (8)$$

where the quantity

$$K = \frac{\lambda_0 \rho c_p}{2(\beta + \alpha n)} \quad (9)$$

depends only on the characteristics of the plate material and is constant in the temperature interval, in which α and β vary only slightly. Obviously, the sensitivity of the system the higher the smaller the value of K.

Expressions (8) and (9) indicate that, measuring the shift of interference fringes, we can unambiguously determine the absolute value of energy density absorbed by the plate over time interval τ:

$$E_{\text{in}}(x, y) = \int_0^\tau Q(x, y)\delta t = \delta N K. \quad (10)$$

Since constant K, which is known for many transparent substances to a high degree of accuracy (and can easily be measured when required), is the only parameter characterizing the system, the thermosensitive interferometer is an absolute instrument that does not require calibration. To determine the power density of incident radiation, we must only divide the measured value of absorbed energy by $(1 - R)$, where R is the reflection coefficient of the interferometer plate at a given wavelength.

The linear expansion coefficient α is always positive for substances we are interested in, while the coefficient describing the temperature variation of the refractive index (see, for example, [10]),

$$\beta \equiv \frac{dn}{dT} = \frac{(n^2 - 1)(n^2 + 2)}{6n}(\Phi - \alpha) \quad (11)$$

can be positive or negative depending on the ratio of the temperature coefficient of polarizability Φ and linear expansion coefficient α. According to the data given in handbooks and on web sites of the manufacturers of optical equipment, the value of β for glass is small and positive, while the value of this parameter for plastics and crystals is positive and large as a rule. The value of K may be an order of magnitude higher than typical values for inorganic glasses, which are quite homogeneous and can easily be processed; however, the optical quality of the surfaces of these materials might create problems after processing. In addition, the thermal and thermooptical parameters of plastics vary to a considerable extent for different samples made of the same material, which requires preliminary measurements. On the other hand, these data for glasses are quite stable to within 2–3%. For the wavelength we are interesting in, K8 glass (or its foreign analog BK7) has a sensitivity factor $K = 5.1 \pm 0.2$ J/cm^2 per fringe (thermal parameters are borrowed from handbook [11]). The above accuracy can serve as an estimate of the overall spread in the data from all available sources.

In the next sections, we will demonstrate the potentialities of the thermosensitive interferometer for measurements in the terahertz range using two examples, viz., the recording of the power density in a terahertz laser beam (using these frames, we will determine the absolute value of radiation power) and visualization of images of the mask covering the beam.

VISUALIZATION OF IMAGES AND DETECTION OF TERAHERTZ RADIATION POWER DENSITY DISTRIBUTION

Measurements were made at a workstation located directly at the exit from the 13-m transport channel. In front of the inlet of the station, the teraherz FEL beam was reflected at an angle of 45° from a spherical metallic mirror with a radius of curvature of 250 cm, forming two focal spots with mutually perpendicular elliptical cross sections as a result of spherical aberration, the glass plate being placed in the first of these cross sections.

Figure 2 shows a series of interference patterns recorded during two seconds after opening of the shutter. The interference pattern shows that the beam power

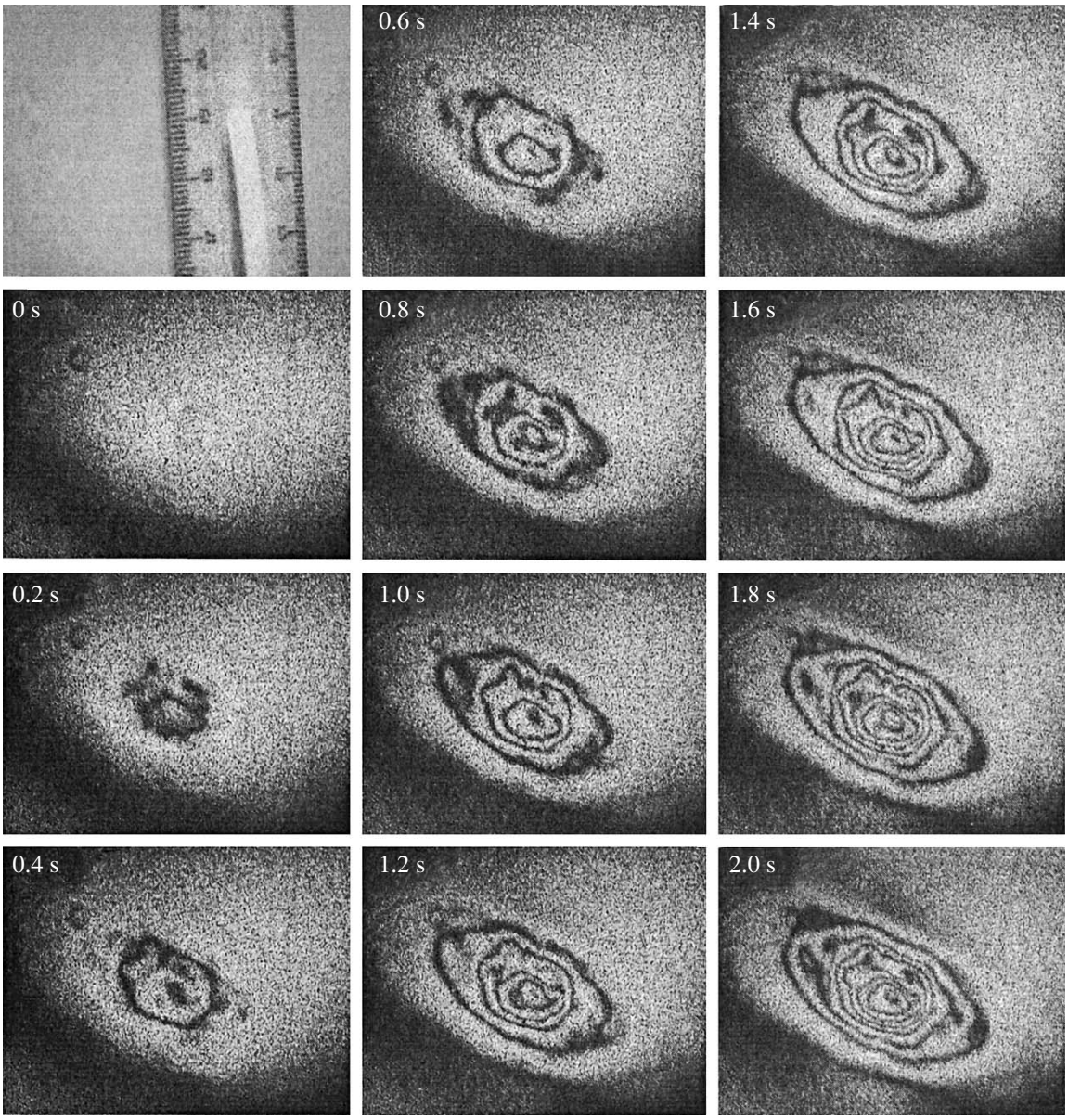

Fig. 2. Images of the laser beam cross section obtained with the help of a thermooptical interferometer; the frame exposure time is 1/25 s; figures indicate the time elapsed from the instant of shutter opening.

density distribution is quite smooth, but still some distortions, which were permanently observed in all interference patterns, can be seen against the background of this distribution. Later, we will discuss whether this structure can depict the actual inhomogeneity of radiation under investigation. The data obtained from qualitative processing of the results will be given below.

Using the interference patterns, we can not only detect broad beams, but also obtain more complicated images. An example is the imaging of a mask (Fig. 3) placed immediately in front of the glass plate of the interferometer. The four frames recorded for a low radiation intensity for 7 s show that the transverse heat flux in the glass plate does not distort significant details of the image with a width of about 3 mm for at least 4 s.

Until now, we ignored the fact that laser radiation consists of a train of short and very intense pulses, which may in principle lead to measuring errors. The thermodynamic processes occurring during the pulse-periodic heating will be discussed in the next section.

PECULIARITIES OF PULSE-PERIODIC RADIATION RECORDING

Radiation emitted by a free electron laser is an infinitely long train of very short pulses ($\tau \approx 50$ ps) separated by long intervals ($T = 1/f \approx 180$ ns) [3]. Conse-

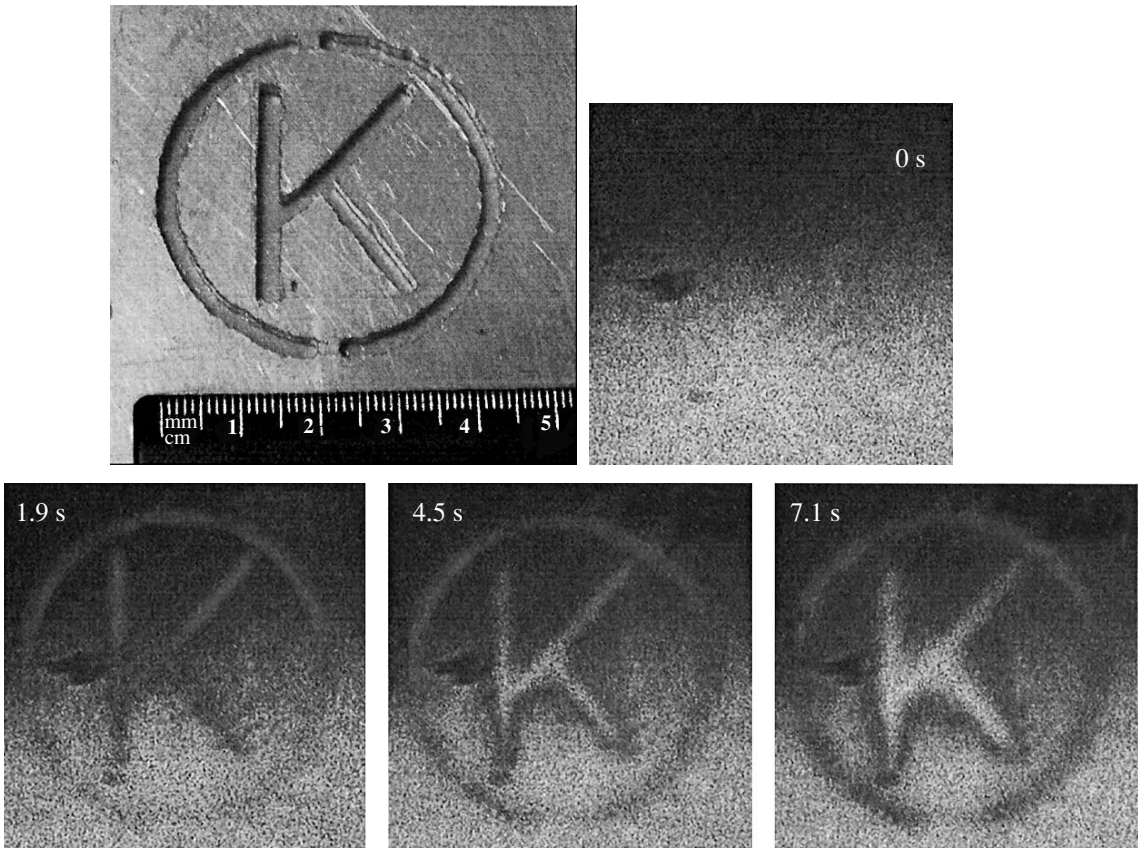

Fig. 3. Image of a terahertz radiation beam transmitted through a shaped aperture in an aluminum screen (whose photograph is shown on top left), recorded with the help of a thermosensitive interferometer; the time elapsed from the instant of shutter opening is indicated on the interference patterns.

quently, for an average power on the order of 100 W, the pulsed power amounts approximately to 350 kW. If the absorption depth of glass for terahertz radiation is very small, we must be sure first of all that the radiation energy per pulse is not spent on glass ablation and that the temperature does not attains values for which thermal radiation carries away a substantial part of the absorbed energy.

It should be stated at the very outset that no visible damage of the surface is observed after a prolonged exposure of the glass plate to terahertz radiation. Let us obtain simple estimates. We first consider the worst case, when the radiation absorption coefficient is infinitely large. In this case, the thickness of the layer heated during a pulse is determined by the diffusion energy transfer coefficient (thermal diffusivity) $a = \kappa/\rho c_p$, where κ is the thermal conductivity; i.e., the energy is absorbed in a layer of thickness $l_1 = (a\tau)^{1/2} \sim 5$ nm. The energy density per pulse for an area of 5 cm^2 and an average beam power of 100 W is $E_1 = 1.8$ μJ/cm^2, which corresponds to an increase in the temperature of this layer by $\Delta T = E_1/l_1\rho c_p = 3.3$ K per pulse. Hence, it is clear that we can disregard thermal radiation emitted from the surface during a micropulse, and ablation is ruled out completely. During the time interval between pulses, the absorbed heat diffuses to a depth $l_2 = l_1(T/\tau)^{1/2} \approx 0.3$ μm, and the excess temperature of the surface decreases by a factor of 50. The process is repeated during next pulses, and the thickness of the heated layer and the temperature averaged over several micropulses increase.

The subsequent diffusion of heat over an interval of the order of seconds can be estimated using the quasi-stationary approximation, in which we disregard the pulse nature of energy supply. The glass plate will be heated to a depth of $l_3 = 0.77$ mm during one second and the increment of the average temperature of the layer amounts to 130 K. The exact solution of the thermal conductivity problem under our conditions (see Appendix) gives values differing by less than 20%. It follows from the estimates that, during the first second, the heated layer can be treated as "one-dimensional" for beams with large cross sections. Since transverse temperature gradients in the heated layer for a broad and sufficiently homogeneous beam are several orders of magnitude smaller than longitudinal gradients (directed along the normal to the surface), the spatial resolution over this time period must constitute hundreds of micrometers.

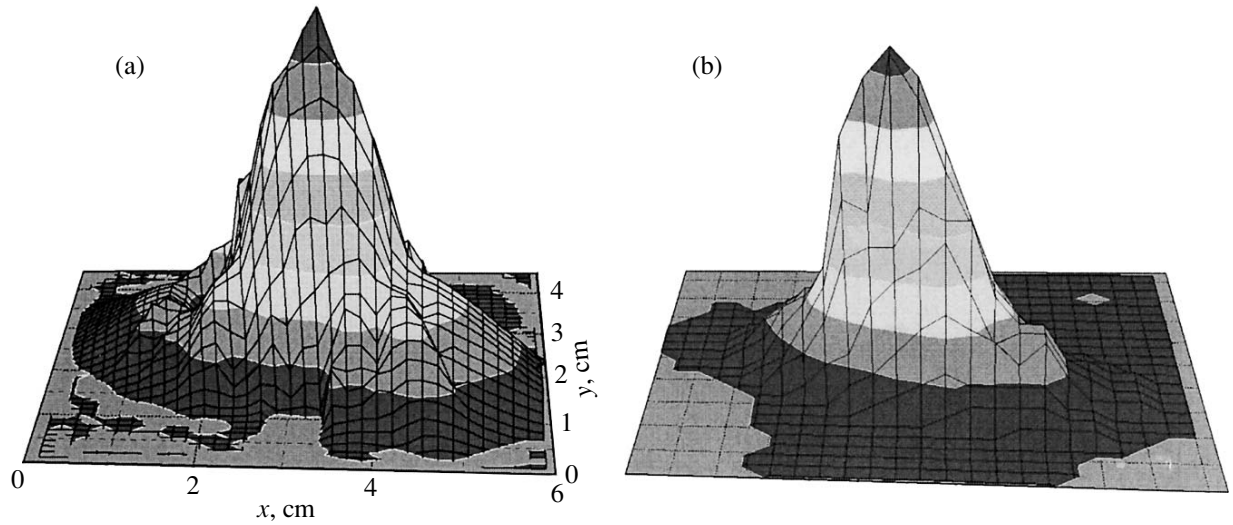

Fig. 4. (a) Distribution of energy density absorbed in a glass plate, reconstructed from the interference pattern recorded at instant $t = 1.6$ s; (b) "temperature" distribution over the glass surface, recorded by a thermograph at instant $t = 0.22$ s.

It can be seen that the scenario described above, which is the worst version of pulse thermal loading, is quite admissible. Indeed, the absorption coefficient measured by us earlier [12] from the intensity for K8 glass in the terahertz range is $K = 860 \pm 30$ cm^{-1}. It follows hence that the radiation absorption depth for a micropulse is $l_1^{\text{rad}} = 1/K = 12$ μm. This value is larger than l_1 and l_2; i.e., the increment of the temperature of the heated (substantially larger) volume is several orders of magnitude smaller than in the case of surface heating, and the thermal conductivity problem should be treated as a problem with a bulk heat source. The numerical solution of this problem (see Appendix) showed that our arguments and estimates (including that of spatial resolution) remain correct over subsecond and second time intervals since $l_1^{\text{rad}} \ll l_3$.

Thus, the calculations confirmed by experiments show that a thermosensitive interferometer can correctly measure the absolute energy of a pulse-periodic terahertz radiation absorbed by a glass plate and can record images with a spatial resolution of fractions of a millimeter for an exposure time of up to one second. To determine the absolute value of energy of incident radiation, we must take into account the energy losses for thermal radiation emitted by the glass surface and for convective cooling. Then we must divide the resultant value by $(1 - R)$, where $R = 0.16$ is the reflection coefficient of glass in the terahertz range (which was also measured in [12]). Since blackbody thermal radiation at a temperature on the order of 420 K amounts to only 0.2 W/cm^2, the losses for the case described here do not exceed 1 W from the entire heated area. Convective heat losses in this case are equal approximately to 0.5 W (see Appendix).

ABSOLUTE MEASUREMENTS OF TERAHERTZ FEL RADIATION

Analysis of thermal processes occurring in a glass screen, which was carried out in the previous section, and high reproducibility of the details of interference patterns in Fig. 2 during 2 s show that a thermosensitive interferometer makes it possible to detect the power density distribution in a terahertz radiation beam with a high spatial resolution. It is well known that the main problem in the processing of interference patterns is the ambiguity in the sign of phase shift. One of the standard solutions, which is also possible in our case, is simultaneous recording of interference patters at two wavelengths. However, we used another method, viz., simultaneous recording of images of a heated region of glass with the help of the SVIT thermograph described earlier. If the temperature increases along a certain direction, the phase advance in the interference pattern is assumed to be positive.

The frequency of image recording by both instruments was 25 frames per second. The terahertz radiation beam was blocked by a shutter. The recording in the thermograph and in the video camera was started immediately before opening of the shutter. Time synchronization was carried out relative to the instant at which the frame with the image appeared, which ensured a lock-on accuracy of 1/25 s.

Figure 4a shows the power density distribution in a terahertz radiation beam absorbed by a glass plate located at the first focus of an inclined spherical mirror. The distribution was reconstructed from the interference pattern recorded at an instant of 1.6 s. The obtained values were normalized to 0.84 to take into account the FEL beam energy reflected from the glass surface. During this period of time, the interferometer operates in a linear mode, which is confirmed by

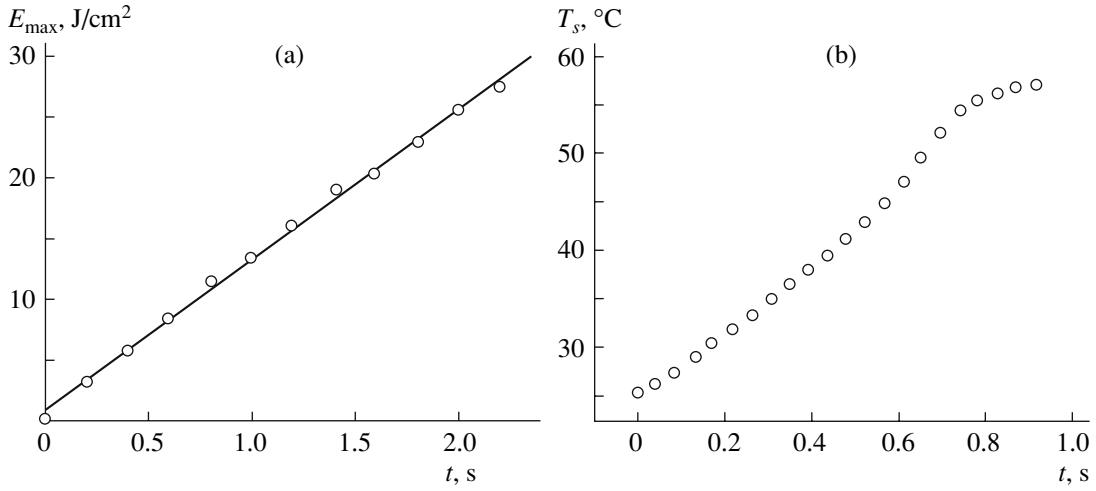

Fig. 5. (a) Increase in the teraherz radiation energy density at the peak of the distribution after opening of the shutter, measured by a thermosensitive interferometer; (b) "temperature" of the heated layer measured by a thermograph as a function of time.

Fig. 5a, demonstrating a linear dependence of the radiation power density at the peak of the time distribution for the entire set of the interference patterns from Fig. 2.

Figure 4b shows the "temperature" distribution over the surface of a glass plate, which was recorded by the thermograph. The range of temperatures being measured has an upper bound at approximately 330 K. At temperatures below this value, the shape of the distribution is very close to that obtained from the interference patterns, which allowed us to unambiguously determine the phase sign on interference patterns in most cases. The phase sign in fine details of the interference pattern could not always be determined correctly in view of a low spatial resolution of the thermograph; however, this did not introduce a significant error in the calculation of the total energy of the terahertz beam.

The "temperature" at the peak of the distribution (Fig. 5b) increases with time at a slightly higher rate than in a linear law, while in the case of blackbody radiation it must increase as a square root of time. This circumstance can be explained by the fact that K8 glass in the sensitivity range of the thermograph matrix (2.5–3.0 μm) is still quite transparent and radiation is emitted not only by the surface, but also by the entire heated layer [13]. Since the thermograph is designed for measuring the temperature of bodies with a high degree of blackness, the absolute values of the scale on the ordinate axis in the figure are given only for reference. A detailed analysis of operation of the thermograph with a glass plate as the screen will be given in a separate publication. In our case, it is important to determine only qualitatively whether the shift of an interference fringe corresponds to the increase or decrease in the wave phase.

The total energy in the terahertz radiation beam incident on the plate was obtained by numerical integration over the volume bounded by the surface (see Fig. 4a). The result of integration gives 17.8/0.85 line/cm^2. Multiplying by $K = 5.1$ J/line, we obtain a value of 105 J over 1.6 s. It was shown above that radiation and convective cooling losses amount to less than 1–2%. Hence, we can conclude that the power of the terahertz free electron laser beam at the exit from the transport channel was $W = 65 \pm 7$ W (taking into account all possible errors).

DISCUSSION

The results of this study indicate high reliability and accuracy of absolute measurements of energy and power density distribution in a terahertz radiation beam by a thermosensitive interferometer. The range of application of the interferometer is naturally not confined to terahertz radiation. This instrument can be used for measuring the power (energy) of any radiation for which the material of the interferometer plate is opaque, as well as for detecting corpuscular flows. Indeed, we successfully used the thermosensitive interferometer for measuring the energy density distribution in an excimer laser beam. In this case, an organic glass plate served as the thermosensitive element. As a rule, plastics have an order-of-magnitude higher sensitivity than that of K8 glass, which makes it possible to measure an order-of-magnitude weaker radiation fluxes.

A certain disadvantage of the method in its above implementation is the long thermal relaxation time of a massive glass plate after a single irradiation. Repeated measurements can be performed approximately 10 min after cooling. This difficulty can be overcome by using a thin (1-mm or thinner) plate that can be intensely cooled from both sides after measurements, although bending of the plate may introduce an error in measurements in this case. A liquid flow screen may be an alternative solution to this problem if the optical inhomogeneity of the flow can be overcome.

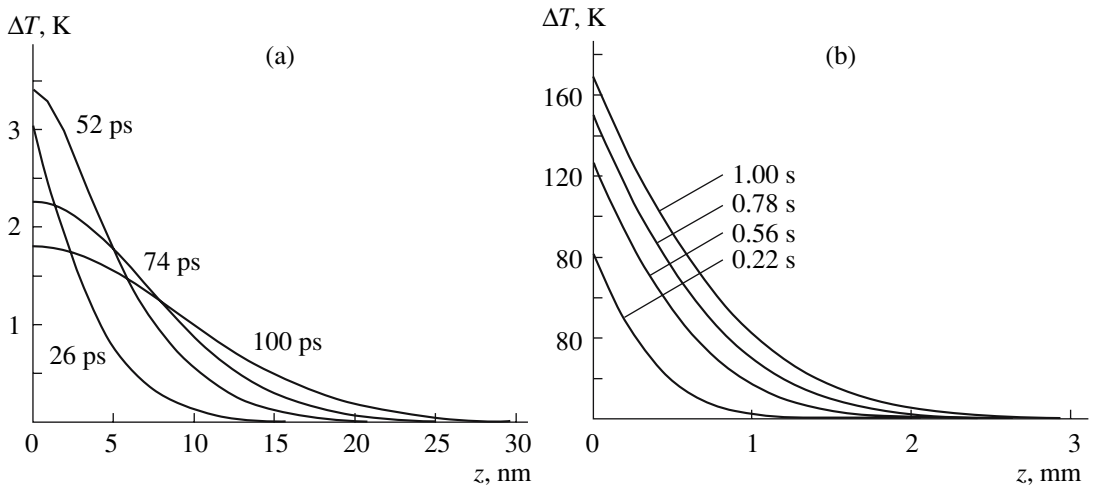

Fig. 6. Calculated temperature distribution in the heated layer (a) during one micropulse and (b) in the subsecond time interval.

Further development of the method will be associated with fast computer-aided reconstruction of the power density distribution from the recorded interference pattern. In spite of numerous publications in this field, we could not find an appropriate program, which would permit the online numerical processing of the interference pattern recorded by a CCD matrix. The main difficulty is associated with the determination of the phase shift sign; the development of the corresponding software would be very helpful. However, these obstacles can be avoided by a slight modification of the experimental setup by recording a shadow pattern with a Foucault knife instead of recording the interference pattern [14]. If we divide the probe laser beam after its passage through the glass plate and the lens by a beam splitter and introduce two mutually perpendicular Foucault knifes into the scheme, two CCD matrices will record the values of $\nabla_{x,y}(\int n(x, y)dz)$ in two mutually perpendicular axes. In this case, numerical reconstruction of the distribution of optical path variation (and, hence, the distribution of energy absorbed by the plate) becomes trivial.

APPENDIX

Numerical and Analytical Calculations of Plate Heating and Cooling Regimes by Pulse-Periodic Radiation

Let us suppose that the radiation absorption length in a substance is very small. As long as the heat penetration depth in the substance is much smaller than the characteristic size of variations of specific power density of incident radiation and the plate thickness, we can use the 1D model of heat propagation in a semi-infinite medium, on whose surface a heat flux varying with time is specified. The temperature in the medium at each instant $T(z, t)$ is described by the equation

$$\frac{\partial T}{\partial t} = a\frac{\partial^2 T}{\partial z^2}, \tag{12}$$

where $a = \kappa/C_p\rho$ is the thermal diffusivity of the substance.

The boundary and initial conditions have the form

$$T_x(0, t) = \varphi(t) = -\frac{P}{\kappa}\psi(t), \tag{13}$$

$$T(z, 0) = 0. \tag{14}$$

The solution to this problem for an arbitrary function $\varphi(t)$ has the form [15]

$$T(z, t) = -\sqrt{\frac{a}{\pi}}\int_0^t \frac{\varphi(t)}{\sqrt{t-\tau}}\exp\left[-\frac{z^2}{4a(t-\tau)}\right]d\tau. \tag{15}$$

Let the source function $\psi(t)$ have the form of unit rectangular pulses of duration $t_1 = 50$ ps with an interval $t_2 = 178.6$ ns between the pulses. On time intervals $[A, B]$ during which $\psi(t) = 1$, a function $\Phi(A, B, t)$ is defined as

$$\Phi(A, B, t) = \int_A^B \frac{1}{\sqrt{t-\tau}}\exp\left[-\frac{z^2}{4a(t-\tau)}\right]d\tau$$

$$= \left\{2\sqrt{t-A}\exp\left[-\frac{z^2}{4a(t-A)}\right] + \sqrt{\frac{\pi}{a}}zErf\left[\frac{z^2}{4a(t-A)}\right]\right\} \tag{16}$$

$$-\left\{2\sqrt{t-B}\exp\left[-\frac{z^2}{4a(t-B)}\right] + \sqrt{\frac{\pi}{a}}zErf\left[\frac{z^2}{4a(t-B)}\right]\right\}.$$

The temperature distribution along the z axis during the first pulse ($0 < t < t_1$) has the form

$$T(z, t) = \frac{P}{\kappa}\sqrt{\frac{a}{\pi}}\Phi(0, t, t). \quad (17)$$

By the end of the pulse, we have

$$T(z, t_1) = \frac{P}{\kappa}\sqrt{\frac{a}{\pi}}\Phi(0, t_1, t_1). \quad (18)$$

In the interval between the first and second pulses ($t_1 < t < t_2$), the temperature is

$$T(z, t_1) = \frac{P}{\kappa}\sqrt{\frac{a}{\pi}}\Phi(0, t_1, t). \quad (19)$$

To determine the temperature at an arbitrary instant, we introduce an integer variable $N = [t/t_2]$ and the residue of division $\delta t = t - Nt_2$; then the solution can be written in the form of the corresponding sum over pulses and the intervals between them. We substitute the known characteristics of K8 glass ($\kappa = 1.11$ W/(m K), $\rho = 2.52$ g/cm^3, and $C_p = 0.86$ J/(g K)). We assume for our estimates that the mean power of terahertz radiation absorbed by glass is $P_0 = 100$ W for an effective exposure area of $S = 5$ cm^2. The dynamics of the temperature increase in the surface layer is shown in Fig. 6a. It can be seen that the values obtained for the temperature increment and the heating depth are in good agreement with the simple estimated obtained above.

The calculation of glass heating for 1 s shows (Fig. 6b) that the characteristic depth of heating amounts to approximately 1 mm, while the temperature of the glass surface increases by 170 K as compared to the initial temperature. The average temperature of the layer increases by 118 K, which is in excellent agreement with the value of 120 K obtained earlier using simple estimates. It should be noted that, for subsecond time intervals, numerical calculations of the dynamics of glass heating in the cases of pulse-periodic and continuous radiation of the same power give completely identical results.

Cooling of the Wall due to Natural Convection

The heat-transfer coefficient for natural convection near a vertical wall [16] is calculated by the formula

$$\alpha = \kappa_0 \frac{0.508}{x\sqrt{2}} Gr^{1/4},$$

where $Gr = (gx^3/\nu^2)(T_{st} - T_0/T_0)$ is the Grashof number. Using tabulated data for thermal conductivity, density, and viscosity of air ($\kappa_0 = 0.034$ W/(K m), $\rho_0 = 1.29$ g cm^3, and $\eta = 1.411 \times 10^{-1}$ cm^2/s) and assuming that the wall temperature is $T_w = 430$ K and the ambient air temperature is $T_0 = 300$ K, we obtain $\alpha = 8.302 \times 10^{-4}$ W/(cm^2 K). Then the heat flux from the wall due to natural convection is $Q = 0.54$ W, while the average laser radiation power absorbed by the wall is $P_0 = 100$ W. The mean velocity of air near the heated wall is $w = 1$ m/s.

ACKNOWLEDGMENTS

The authors are grateful to A.A. Pavlov and V.M. Boiko, who attracted our attention to the possibility of using a thermosensitive interferometer, as well as to V.V. Kotenkov, V.V. Kubarev, T.V. Salikova, and S.S. Serednyakov for discussions and assistance in experiments.

This study was partly financed by the Integration grant nos. 174/6 and 22/6 from the Siberian Division of the Russian Academy of Sciences and by the Ministry of Education and Science of the Russian Federation (grant no. RNP.2.1.1.3846).

REFERENCES

1. S. P. Mickan and X.-C. Zhang, Int. J. High Speed Electron. Syst. **13**, 601 (2003).
2. A. Gurtler, A. S. Meijer, and W. van der Zande, J. Appl. Phys. Lett. **83**, 222 (2003).
3. V. P. Bolotin, N. A. Vinokurov, D. A. Kayran, et al., Nucl. Instrum. Methods Phys. Res. A **543**, 81 (2005).
4. J. Nishizawa, K. Suto, T. Sasaki, et al., J. Phys. D **36**, 2958 (2003).
5. B. Vainer, in *Proceedings of the 5th Conference on Quantitative Infrared Thermography (QIRT-2000), Eurotherm Seminar 64, Reims, France, 2000*, p. 84.
6. V. P. Aksenov and N. Yu. Isaev, Opt. Atmos. Okeana **5**, 841 (1992).
7. N. Yu. Isaev and E. V. Zakharova, Opt. Atmos. Okeana **8**, 509 (1995).
8. M. P. Golubev, A. A. Pavlov, Al. A, Pavlov, and A. N. Shiplyuk, Prikl. Mekh. Tekh. Fiz. **44**, 174 (2003).
9. P. Hariharan, in *Handbook of Optics*, Vol. 2: *Devices, Measurements and Properties*, Ed. by M. Bass (McGraw-Hill, New York, 1995), p. 21.1.
10. E.-S. Kang, T.-H. Lee, and B. S. Bae, Appl. Phys. Lett. **81**, 1438 (2002).
11. M. Ya. Kruger, V. A. Panov, V. V. Kulagin, *A Handbook for the Designer of Optomechanical Devices* (Mashinostroenie, Leningrad, 1967) [in Russian].
12. V. V. Gerasimov, B. A. Knyazev, P. D. Rudych, and V. S. Cherkasskiĭ, Preprint No. 2006-23, IYaF SO RAN (Institute of Nuclear Physics, Siberian Division, Russian Academy of Sciences, Novosibirsk, 2006).
13. N. A. Rubtsov, *Heat Exchange by Radiation (Heat Exchange in Systems with Radiating and Attenuating Media)* NGU, Novosibirsk, 1980 [in Russian].
14. M. M. Skotnikov, *Quantitative Shadow Methods in Gas Dynamics* (Nauka, Moscow, 1976) [in Russian].
15. B. M. Budak, A. A. Samarskii, and A. N. Tikhonov, *A Collection of Problems on Mathematical Physics* (Nauka, Moscow, 1980; Pergamon, Oxford, 1964).
16. S. N. Shorin, *Heat Transfer* (Vysshaya Shkola, Moscow, 1964) [in Russian].

Translated by N. Wadhwa